Simple, compact, high-performance permanent-magnet Faraday isolator

Daniel J. Gauthier, Paul Narum, and Robert W. Boyd

Institute of Optics, University of Rochester, Rochester, New York 14627

Received May 1, 1986; accepted July 21, 1986

The design of a Faraday isolator that uses a short glass rotator rod and produces highly uniform rotation across its clear aperture is presented. The rotator rod is 19.5 mm long, and at a wavelength of 633 nm the rotation angle is 45 deg and the isolation ratio is >45 dB.

Faraday isolators are important components of many laser systems. In order to provide good isolation and high transmission, it is necessary that the polarization direction of the incident light be rotated by 45 deg in passing through the rotator portion of the isolator. Until recently, such a degree of rotation was possible only for wavelengths[1] greater than 5 μm or through the use of cooled[2] or pulsed[3] electromagnets. However, the recent availability of paramagnetic glasses with large Verdet constants[4] and strong permanent magnets[5] has permitted the construction of permanent-magnet Faraday rotators.[6] The length of the glass element of such a device should be as short as possible in order to minimize absorption losses, to increase the threshold for self-focusing, and to reduce the cost of the magnets and glass. We present the design of a permanent-magnet Faraday rotator that is both simple and compact. In particular, our design gives better isolation and uses a shorter glass path length than two recently published designs[7,8] and does not require the use of compensator plates,[8] even though our design utilizes magnets of similar strength and glass of similar Verdet constant.

The design that we consider is shown in Fig. 1(a). The magnets are right-circular cylinders of diameter $2b$ with a concentric hole of diameter $2a$ and are assumed to be uniformly magnetized with magnetization $\mathbf{M}$. The length L_r of the glass rotator rod is nearly equal to the length L of the central magnet. An additional magnet of length L' is placed at each end of the central magnet with its magnetization vector oriented antiparallel to that of the central magnet. Previous studies[7] have shown that the rotation of the device is increased through use of these auxiliary magnets.

The rotation angle Θ introduced by a single pass through the Faraday rotator is given by

$$\Theta = V \int H_z dz , \tag{1}$$

where V is the Verdet constant, H_z is the axial component of the magnetic intensity vector, and the integration is to be performed over the length of the rotator rod. Since the free current density is equal to zero in our case, the magnetic field can be described in terms of a scalar potential Φ defined through the relation $\mathbf{H} = \nabla\Phi$. Note that the rotation angle Θ given by Eq. (1) can be represented as the product of the Verdet constant and the difference in the scalar potential at the two ends of the rotator rod. From the Maxwell equations $\nabla \cdot \mathbf{B} = 0$ and $\nabla \times \mathbf{H} = 0$ and the constitutive relation $\mathbf{B} = \mathbf{H} + 4\pi\mathbf{M}$, it can be readily seen that

$$\nabla^2\Phi = 4\pi\nabla \cdot \mathbf{M} . \tag{2}$$

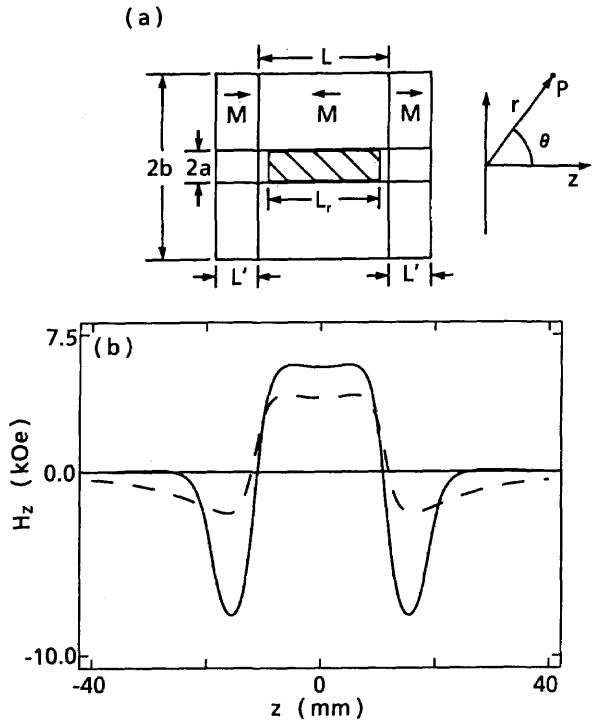

Fig. 1. (a) Cross-sectional view of the permanent-magnet Faraday isolator. The rotator rod of length L_r is located at the center of a hole of diameter $2a$ in a magnetic stack. The stack is composed of a central magnet of length L and two auxiliary magnets of length L' whose magnetization is antiparallel to that of the central magnet. The coordinate system is used in the calculation presented in the text. (b) The axial component of the magnetic intensity produced by the magnetic stack as a function of position along the symmetry axis. The dashed curve shows the field in the absence of the two auxiliary magnets.

0146-9592/86/100623-03$2.00/0

For a right-cylindrical permanent magnet with uniform magnetization along its axis, $\nabla \cdot \mathbf{M}$ vanishes everywhere except on the pole faces. We solve Eq. (2) using a spherical coordinate system whose origin is at the center of the pole face and whose polar axis is normal to the pole face, as shown in Fig. 1(a). The potential due to each pole face obeys Laplace's equation $\nabla^2\Phi = 0$ and hence can be represented as[9]

$$\Phi(r, \theta) = \int_{l=0}^{\infty} [A_l r^l + B_l r^{-(l+1)}] P_l(\cos\theta) \qquad (3)$$

everywhere except on the pole face. In this equation, $P_l(\cos\theta)$ is the Legendre polynomial of order l. The coefficients A_l and B_l are determined by requiring that the solution (3) coincide with the potential on axis, which is determined straightforwardly by using the Green's function method to be of the form

$$\Phi(r, \theta) = \int_0^R \int_0^{2\pi} \frac{M r' \mathrm{d}r' \mathrm{d}\phi'}{(r'^2 + r^2)^{1/2}} = 2\pi M[(r^2 + R^2)^{1/2} - r], \qquad (4)$$

where R is equal to the radius of the pole face. When r is less than R, we expand Eq. (4) in a power series in r/R and match the coefficients of terms with equal powers of r in Eq. (3) to obtain the equation for the potential:

$$\Phi(r, \theta) = 2\pi M\left[R - r\cos(\theta) + R \times \sum_{l=0}^{\infty} \frac{P_{2(l+1)}(\cos\theta)(2l)!(-1)^l}{2^{2l+1} l!(l+1)!}\left[\frac{r}{R}\right]^{2(l+1)}\right], \quad r < R. \qquad (5)$$

Similarily, for $R < r$ we expand Eq. (4) in a power series in R/r and obtain

$$\Phi(r, \theta) = 2\pi M r \sum_{l=0}^{\infty} \frac{P_{2l}(\cos\theta)(2l)!(-1)^l}{2^{2l+1} l!(l+1)!}\left[\frac{R}{r}\right]^{2(l+1)}, \quad r > R. \qquad (6)$$

For points on the symmetry axis, the potential for the entire magnet stack is obtained by superposing the potential due to each pole face as given by Eq. (4) to obtain

$$\Phi(z, 0) = 2\pi M[2(z_1^2 + a^2)^{1/2} - 2(z_1^2 + b^2)^{1/2} + 2(z_2^2 + a^2)^{1/2} 2(z_2^2 + b^2)^{1/2} + (z_3^2 + b^2)^{1/2} - (z_3^2 + a^2)^{1/2} + (z_4^2 + a^2)^{1/2} - (z_4^2 + b^2)^{1/2}], \qquad (7)$$

where $z_1 = z - L/2$, $z_2 = z + L/2$, $z_3 = z - L/2 - L'$, and $z_4 = z + L/2 + L'$ and where the origin is now located at the center of the central magnet.

Our design of a simple and compact Faraday rotator is shown in Fig. 1(a) with $a = 2.8$ mm, $b = 16.5$ mm, $L = 22.8$ mm, $L_r = 19.5$ mm, and $L' = 7.6$ mm. The magnets[10] are Sm_2Co_{17} permanent magnets with residual magnetic induction of 10^4 G. The rotator glass[11] contains the paramagnetic ion terbium and has a Verdet constant of -4.12 deg/kOe cm at a wavelength of 633 nm. The Verdet constant scales approximately as λ^{-2} for other wavelengths. The value of the magnetic field on axis is obtained through differentiation of Eq. (7) and is shown plotted as a function of z in Fig. 1(b).

For comparison, we also show the on-axis field in the absence of the auxiliary magnets. The auxiliary magnets are seen to increase the field in the region of the rotator rod, and hence to increase the rotation, by approximately 40%. In the limit of infinitely long auxiliary magnets, the rotation is enhanced by a factor of 2, as can be seen from Eq. (7).

Figure 2 shows how the integrated on-axis magnetic intensity, and hence the rotation, scales with our free design parameters L, L', and b while holding the inner radius a constant at 2.8 mm. We have also assumed that the length L of the central magnet is equal to the length L_r of the rotator rod, because L is approximately equal to L_r in an optimized design and because the rotation depends rather insensitively on L for $L \approx L_r$, as can be seen from Fig. 3. This figure also shows how the nonuniformity of the rotator depends on the length L of the central magnet. The nonuniformity is defined to be the fractional difference in rotation on axis and at a radial distance of 2.5 mm. We have determined that the fractional difference scales nearly quadratically with the radial distance. Note that the

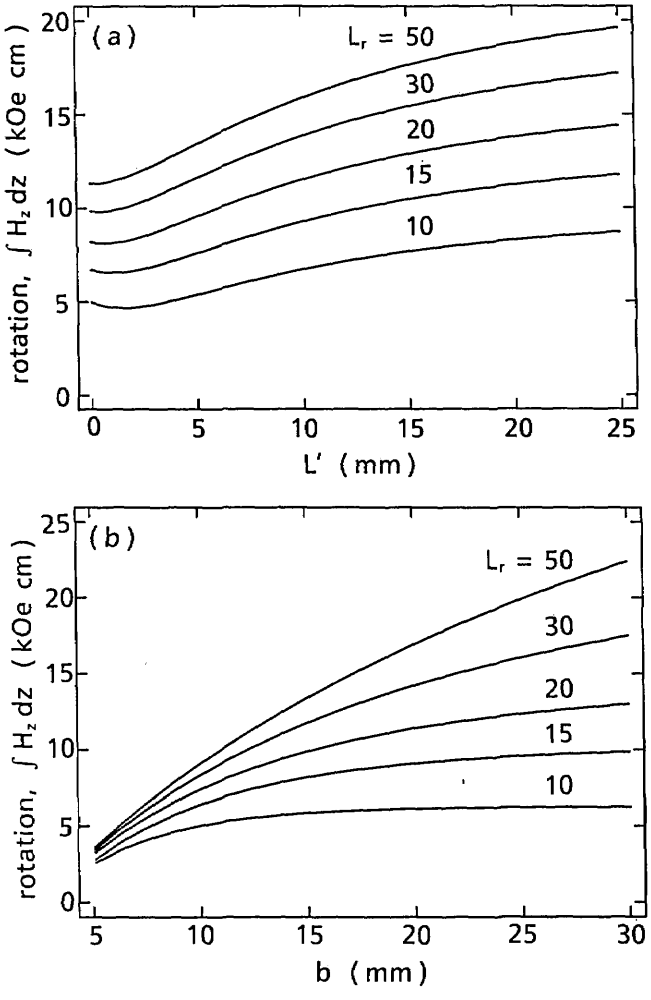

Fig. 2. Integrated on-axis magnetic intensity (proportional to the rotation) (a) as a function of the length L' of the auxiliary magnet for $b = 16.5$ mm and (b) as a function of the radius b of the magnets for $L' = 7.6$ mm, for various values of the rod length L_r, which is held equal to the length L of the central magnet. In both cases, the radius of the hole is $a = 2.8$ mm and the residual inductance is 10^4 G.

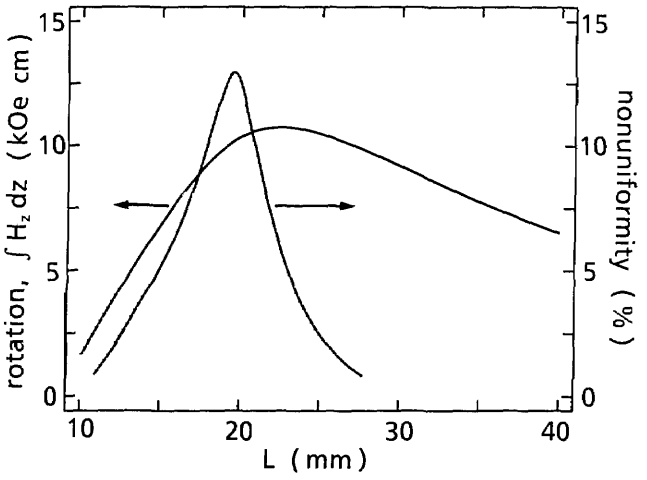

Fig. 3. Integrated on-axis magnetic intensity and fractional difference in the rotation angle between the axis and at a distance of 2.5 mm from the axis as a function of the length L of the central magnet. The length of the rotator rod is held fixed at 19.5 mm, and $a = 2.8$ mm, $b = 16.5$ mm, $L' = 7.6$ mm, and the residual inductance is equal to 10^4 G.

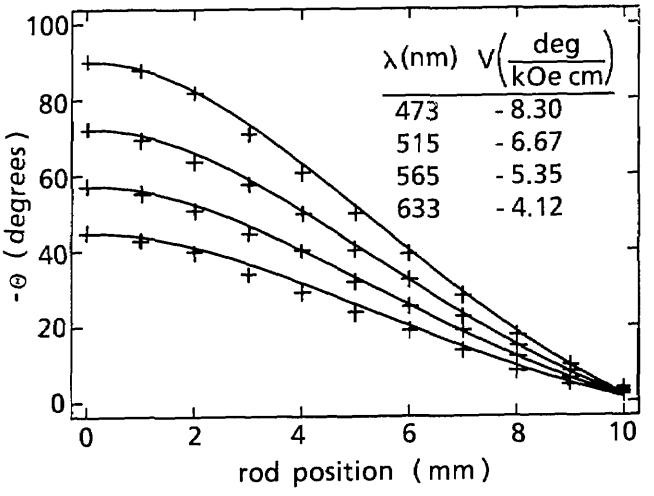

Fig. 4. Measured rotation angle as a function of the displacement of the rotator rod from its central position for various wavelengths given in the legend. At any position, the rotation decreases with increasing wavelength. The solid lines are theoretical curves calculated using the tabulated value of the Verdet constant.

nonuniformity depends on L much more strongly than does the rotation. Hence by choosing L to be slightly greater than L_r we can achieve dramatically improved uniformity with only a small change in rotation. We find that for $b \gg a$ the nonuniformity can be reduced to below 2% by increasing the length of the central magnet until the on-axis rotation is reduced to 95% of its value when L is equal to L'.

Through use of Figs. 2 and 3, one can optimize the performance of a permanent-magnet Faraday rotator. As an example, our design criteria were that the rotation angle be 45 deg at a wavelength of 633 nm, that the diameter of the clear aperture be 5 mm, and that the isolation ratio be greater than 43 dB for a Gaussian beam of diameter 2 mm. An isolation ratio of 43 dB corresponds to a maximum radial change of rotation of 5% over the 5-mm clear aperture. For the Verdet constant of our glass, an integrated magnetic intensity of 10.8 kOe cm is necessary to meet the rotation requirement. It can be seen from Figs. 2 and 3 that our design meets these criteria.

We have built the Faraday rotator described above and find that its performance characteristics are well described by our theoretical model. Figure 4 shows how the rotation angle varies as the rotator rod is displaced from the center of the magnet stack for several different wavelengths. The solid lines are theoretical predictions, using the tabulated values of the Verdet constant[11] that are presented in the legend to the figure. Note that a rotation of 45 deg can be obtained for wavelengths shorter than 633 nm by such a displacement of the rotator rod. We have calculated the nonuniformity in rotation across the clear aperture for a displaced rod and find that it is less than 5% for all positions that are shown in Fig. 4. The measured value for the change in rotation across the aperture is found to be within a few percent of the theoretically predicted value. At a wavelength of 515 nm, the radial nonuniformity at the position of the rotator that gives 45-deg rotation is calculated and measured to be less than 2%. At this wavelength, the isolation ratio is found to be 47 dB when the Faraday rotator is placed between two high-quality calcite polarizers.[12] The insertion loss at 515 nm is 0.8 dB, of which 0.63 dB is due to reflection losses from the uncoated surfaces of the rotator rod.

In conclusion, we have presented the design of a Faraday isolator that is simple and compact and that produces extremely good isolation using a glass path length shorter than that of previous designs.

References

1. S. D. Jacobs, K. J. Teegarden, and R. K. Ahrenkeil, Appl. Opt. **13**, 2313 (1974); H. C. Meyer, G. A. Tanton, S. S. Mitra, and J. D. Stettler, Appl. Phys. **13**, 307 (1977); F. Keilmann, R. L. Sheffield, M. S. Feld, and A. Javan, Appl. Phys. Lett. **23**, 612 (1973).
2. L. J. Aplet and J. W. Carson, Appl. Opt. **3**, 544 (1963); L. G. DeShazer and E. A. Maunders, Rev. Sci. Instrum. **38**, 248 (1967).
3. C. F. Padula and C. G. Young, IEEE J. Quantum Electron. **QE-3**, 483, (1967); O.C. Barr, J. M. McMahon, and J. B. Trenholme, IEEE J. Quantum Electron. **QE-9**, 1124 (1973); P. J. Brannon, F. R. Franklin, G. C. Hauser, J. W. Lavasek, and E. D. Jones, Appl. Opt. **13**, 1555 (1974).
4. N. F. Borrelli, J. Chem. Phys. **44**, 3289 (1964).
5. J. J. Becker, J. Appl. Phys. **41**, 1055 (1970).
6. H. Iwamura, S. Hayashi, and H. Iwasaki, Opt. Quantum Electron. **10**, 398 (1978); F. J. Sansalone, Appl. Opt. **10**, 2329 (1971).
7. K. P. Birch, Opt. Commun. **43**, 79 (1982).
8. K. Shiraishi, F. Tajima, and S. Kawakami, Opt. Lett. **11**, 82 (1986).
9. J. D. Jackson, *Classical Electrodynamics* (Wiley, New York, 1975), Sec. 3.3.
10. Electron Energy Company, P.O. Box 458, Landisville, Pa. 17538.
11. Kigre, Inc., 5333 Secor Road, Toledo, Ohio 43623.
12. Karl Lambrecht Company, 4202 North Lincoln Avenue, Chicago, Ill. 60618.